Journal of Materials Chemistry C

Accepted Manuscript

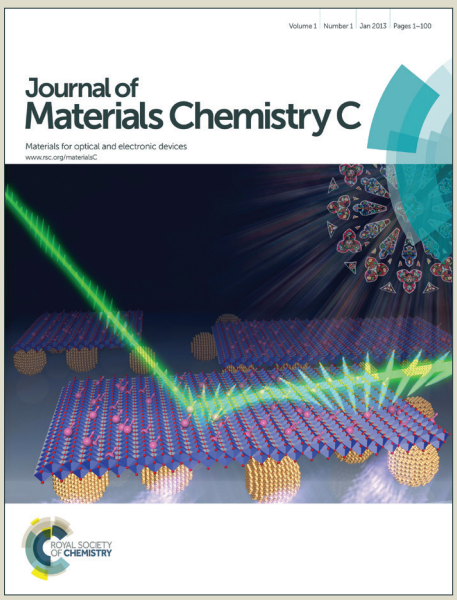

ROYAL SOCIETY OF CHEMISTRY

www.rsc.org/materialsC

Manuscript submitted to *Journal of Materials Chemistry C*

Supramolecular P4VP-Pentadecylphenol Naphthalenebisimide Comb-Polymer: Mesoscopic Organization and Charge Transport Properties.

***Rekha Narayan*[a], *Prashant Kumar,*[d] *K. S. Narayan*[d] and *S. K. Asha**[a,b,c]

a) Polymer Science and Engineering Division, CSIR-National Chemical Laboratory, Dr Homi Bhabha Road, Pune 411008, India.
b) Academy of Scientific and Innovative Research, New Delhi, India
c) CSIR-Network Institutes of Solar Energy, New Delhi, India
d) Chemistry and Physics of Material Unit, Jawaharlal Nehru Centre for Advanced Scientific Research Jakkur, Bangalore - 560064, Karnataka, India

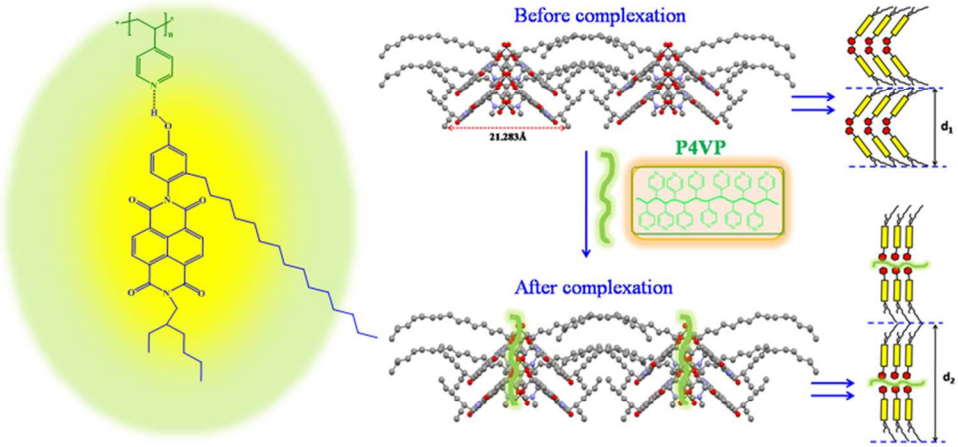

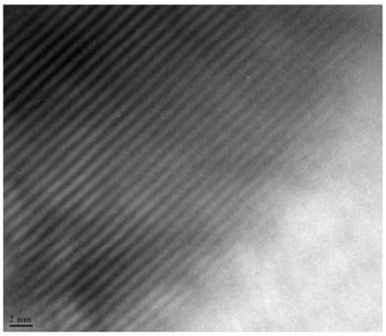

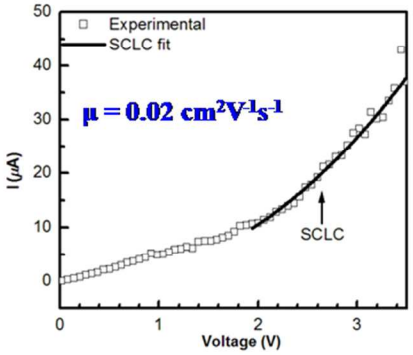

Corresponding Author: S. K. Asha, E-mail: sk.asha@ncl.res.in Fax: 0091-20-25902615.

Abstract:

A supramolecular comb polymer of Pentadecyl Phenol (PDP) substituted Naphthalenebisimide (**PDP-UNBI**) with poly(4-vinylpyridine) (P4VP) is reported. The mesoscopic organization within the **P4VP(PDP-UNBI)$_n$** complexes were studied using wide angle X-ray diffraction (WXRD) techniques. The packing diagram obtained from the single crystal XRD analysis of the **PDP-UNBI** crystals gave a clear picture of the initial arrangement present in the self-associated **PDP-UNBI** alone. Correlating this with the XRD data of the hydrogen bonded polymer complex provided insight into the probable packing of the P4VP chains within the crystalline lattice of **PDP-UNBI** leading to a highly ordered lamellar packing. Transmission electron microscopy (TEM) revealed the uniform mesomorphic lamellar structures in the domain range of ~ 5-10 nm. Furthermore, the charge carrier mobility measurements observed from space charge limited current (SCLC) measurements demonstrated that transport behaviour of the hydrogen bonded **P4VP(PDP-UNBI)** complex (2 x 10^{-2} cm^2/Vs) was comparable to that of the crystalline naphthalene bisimide molecule itself (9 x 10^{-3} cm^2/Vs), which is a great achievement since the complex now offered a package of solution processable n-type semiconductor polymer with mobility equivalent to that of a crystalline small molecule.

Keywords: Naphthalenebisimide, P4VP, supramolecular-polymer, hydrogen-bonding, single crystals, lamellar nanostructures

Introduction

Materials research in the past few years has witnessed a tremendous growth in the search for new n-type organic semiconductor materials that can compete with the device performances exhibited by already well established p-type semiconductors. Organic p-type semiconductors based on a series of benzothiophene derivatives exhibiting high hole mobility values even upto 31.3 cm^2/Vs has been reported by Hasegawa *et al*.[1, 2] However, organic n-type semiconductors with electron mobilities higher than 1.0 cm^2/Vs still remain limited. Currently the most extensive studies on non-fullerene category of n-channel organic materials are based on the rylene diimide cores viz., perylene and naphthalene diimides. Eventhough outstanding results are obtained with vacuum deposited thin films of the rylene molecules, fully solution processable polymeric derivatives are scarce. Among the rylene family of electroactive compounds, naphthalenebisimide derivatives have attracted a great deal of attention because of their high crystallinity, good self assembling characteristics, high electron affinity and field effect mobilities.[5-7] Apart from their applications in organic electronics and more particularly in the fabrication of n-channel field effect transistors,[8-11] they have also been extensively used as supramolecular building blocks of functional materials such as organogels,[12, 13] liquid crystals,[14, 15] foldamers,[16, 17] catenanes,[18, 19] nanotubes [20, 21] etc. Small molecule based NBI derivatives have proved to be among the best performing n-type organic semiconductors known so far.[22-24] Although there are reports on naphthalenebisimide based polymeric materials, a vast majority of them are donor-acceptor type main-chain copolymers with different donor monomers and NBI as the acceptor monomer in a conjugated fashion designed to alter the electronic properties suitably for optoelectronic applications.[4, 25-32] Compared to main-chain polymers, naphthalenebisimide based side-chain polymer reports are very less or rare.

A key issue regarding the development of polymeric semiconductor materials for organic electronics applications is the innovation of rational design and control of easily accessible novel polymer architectures by simple, smart strategies which are capable of performing crucial functions. Strategies that can build ordered structures with tailor-made optical, electronic and mechanical properties are in high demand for material science. Functional comb polymer architecture via a modular approach created by attaching short chain molecules (amphiphiles or surfactants) through physical interactions to either a homopolymer [33] or to one of the blocks of a di-block copolymer, are well known to form mesomorphic structures, as reported in the

extensively studied P4VP-PDP based non-covalent surfactant-polymer system by Ikkala and ten-Brinke and later on by others.[34-36] Recently, we reported well defined nano organization of n type semiconductors based on perylenebisimide with the polymer poly(4-vinyl pyridine) (P4VP), resulting in lamellar structures in the domain range of 5-10 nm with a clear trend of higher conductance compared to the pristine PBI molecule.[37] Considering the importance and performance of the lower member of the rylenebisimides family namely the naphthalenebisimides (NBI) in the field of n-type organic semiconductors, this work highlights our study of the supramolecular comb polymer based on Pentadecyl Phenol functionalized naphthalenebisimide (**PDP-UNBI**) with poly(4-vinyl pyridine) P4VP mediated by hydrogen bonding interactions. It was envisaged that polymeric n-type semiconductor materials with high electron mobility could be obtained using this concept. The complex formation between **PDP-UNBI** and P4VP was confirmed by means of FT-IR and ^{1}H-NMR spectroscopic methods. The solid state packing of the mesogens in the bulk structure was analyzed in detail using X-ray diffraction techniques (WXRD). Additionally more light was shed on the packing nature of the complexes utilizing the single crystal analysis of **PDP-UNBI**. Transmission microscopy (TEM) imaging was used for probing the visual evidence for the mesomorphic morphologies. Finally the charge transport properties of the complexes were investigated by SCLC method. The set of fundamental studies presented here pave pathways toward simple and smart polymeric functional materials that can serve as precursors of well organized hybrid nanocomposites for optoelectronic applications.

Experimental Section

Materials:

Poly(4-vinylpyridine) (P4VP) (Mw =60,000) was purchased from Aldrich. It was dried in vacuum oven at 60 °C for 3 days prior to use. The other starting materials naphthalenetetracarboxylic acid dianhydride (NTCDA), 2-ethyl-1-hexyl amine, 3-pentadecylphenol and other reagents were also purchased from Aldrich and used without any further purification. All solvents used were of analytical grade and carefully dried before use according to standard procedures.

Instrumentation Details: ^{1}H and ^{13}C-NMR spectra were recorded in $CDCl_3$ using Bruker AVENS 200 MHz spectrophotometer. MALDI-TOF analysis was carried out on a Voyager-De-

STRMALDI-TOF (Applied Biosystems, Framingham, MA, USA) instrument equipped with 337 nm pulsed nitrogen laser used for desorption and ionization. Size exclusion chromatography (SEC) in THF was done using polystyrene standards for calibration. Infrared spectra were obtained using Bruker α-T spectrophotometer in the range of 4000-400 cm^{-1}. All the complexes were directly solution drop cast onto KBr pellets and solvent evaporated off slowly at 60-70 °C, followed by drying in vacuum oven overnight. Thermogravimetric analysis (TGA) was performed using a PerkinElmer STA 6000 thermogravimetric analyser. DSC (differential scanning calorimetry) measurements were performed on TA Q10 differential scanning calorimeter at a heating rate of 10 °C/min under nitrogen atmosphere. Typically, 3-4 mg of samples was placed in an aluminum pan, sealed properly and scanned from -50°C to 250 °C. The first heating cycles were avoided to get rid of thermal history of the samples. Wide Angle X-ray Diffractograms (WXRD) were obtained using a Philips analytical diffractometer with CuKα emission. All the samples were recorded in the (2θ) range of 3–50 degrees using a PANalytical X'pert Pro dual goniometer diffractometer and analyzed using X'pert software. An X'celerator solid-state detector was employed in wide-angle experiments. The radiation used was CuKα (1.54 Å) with a Ni filter, and the data collection was carried out using a flat holder in Bragg–Brentano geometry. Single crystals were subjected to data collection at 100 K on a Bruker APEX duo CCD-X-ray diffractometer equipped with graphite monochromated Mo Ka radiation (λ = 0.71073 Å). The frames were integrated with a Bruker APEX software package. The structures were solved by direct methods and refined with a full matrix least-squares technique using SHELX S v97 programs. The optical microscope images of the single crystals were taken on a LEICA DM2500 polarized light microscope, attached with a digital camera. Transmission Electron microscopy (TEM) was done using an FEI-Tecnai^{TM}-F20 electron microscope operating at 200 kV. Sandwich structures on Indium tin oxide (ITO) coated glass and Aluminium substrates were fabricated for the SCLC studies. Thin films of the samples were drop-cast from chloroform and spin coated on the substrates. The thickness was determined using Dektak surface profiler. The top Al electrode defining the area of the film (0.1 cm^2) was coated using thermal deposition method in high vacuum. All measurements were carried out under inert atmosphere.

Sample preparation: The unsymmetrical amphiphilic naphthalenebisimide (**PDP-UNBI**) and Poly (4-vinylpyridine) (P4VP) were dried in vacuum oven at 60 °C for 3 days. **P4VP(PDP-**

UNBI)$_n$ complexes were prepared from dry $CHCl_3$ solutions, where 'n' denotes the number of PBI molecules per vinyl pyridine (VP) repeat unit (n= **PDP-UNBI** /VP). In a typical procedure P4VP was first dissolved in $CHCl_3$ to which desired amount of **PDP-UNBI** was added depending on the value of 'n' and the solution was stirred for 24 hours under nitrogen atmosphere. Concentration of the solutions was kept as low as 1 wt%. Subsequently the solvent was evaporated slowly on a hot plate at 45 °C and the complexes were further dried in vacuum oven at 40 °C for 3 days, slowly cooled to room temperature and stored in dessiccator thereafter.

Results and Discussion

Supramolecular P4VP(PDP-UNBI)$_n$ Comb polymers

The pentadecylphenol based unsymmetrical naphthalenebisimide (**PDP-UNBI**) was synthesized by simultaneous coupling of 4-amino-3-pentadecylphenol and 2-ethylhexylamine in a one-pot synthesis with Naphthalene-1,4,5,8-tetracarboxylic dianhydride in presence of molten imidazole as reagent. The **PDP-UNBI** was obtained in extremely pure form by repeated column chromatography purification procedures. The details of the synthesis and characterization are given in the supporting information. **PDP-UNBI** was stoichiometrically complexed with P4VP; hydrogen-bond between the pyridine and phenol groups being the mode of non-covalent attachment. The **PDP-UNBI** based supramolecular homo-comb polymers were named as **P4VP(PDP-UNBI)$_n$** where 'n' denoted the number of surfactant molecules per vinyl pyridine repeat unit and this ratio was varied from 0.25 to 1.00. Scheme-1 depicts the chemical structure of the **P4VP(PDP-UNBI)$_{1.0}$** supramolecular comb-polymer. All the supramolecular comb polymers discussed in this study were prepared by solution mixing and evaporation technique, in which the hydrogen bond donor **PDP-UNBI** was dissolved in chloroform to which desired amounts of P4VP in the same solvent were added and the mixture was stirred under inert atmosphere for one day to ensure homogenized hydrogen bond formation nominally. Finally slow evaporation of the solvent yielded the microphase separated supramolecular comb-polymer complexes.

Evidence for Hydrogen-bonding in the Complexes - FT-IR and ^{1}H-NMR Characterizations

Upon hydrogen bond formation with amphiphiles several bands of free pyridine ring of P4VP undergoes shift to higher wavenumbers, as a result of the change in electronic distributions. As

extensively studied in numerous literature examples, the bands of particular interest are 1597 (+6), 1413 (+6) and 993 (+15), where the values in brackets denotes the typical shifts observed for hydrogen bonding interaction.[35-40] The complete FT-IR spectra recorded from 4500 to 600 cm^{-1} for the pure constituents namely P4VP and **PDP-UNBI** are given in figure-1.

It could be seen that the peaks around 992 and 1413 cm^{-1} present in pure P4VP were absent in pure **PDP-UNBI**, but both the constituents had strong bands around 1598 cm^{-1}. Consequently the peaks at 992 and 1413 cm^{-1} were used for tracing the hydrogen bonding interaction in all the complexes. In the case of **P4VP(PDP-UNBI)$_{1.0}$** these peaks showed a shift to 1007 and 1421 cm^{-1} respectively as visible from the scale enlarged FT-IR spectra given in figure-2(a) & (b). This gave evidence for the successful hydrogen bonding of phenol group of **PDP-UNBI** to pyridine unit of P4VP and thus the formation of **P4VP(PDP-UNBI)$_{1.0}$** supramolecule was confirmed. It was also noted that the relative intensities of the hydrogen bonded pyridine band at 1007 cm^{-1} increased systematically as the chromophore content was increased from 25 % to 100 % with concomitant steady vanishing of free pyridine band at 993 cm^{-1}. Similarly there was a gradual shift in the 1413 cm^{-1} band on moving from **P4VP(PDP-UNBI)$_{0.25}$** to **P4VP(PDP-UNBI)$_{1.0}$** (supporting info figure-S.6. (a) & (b)). The supramolecular interaction between the **PDP-UNBI** and P4VP in the **P4VP(PDP-UNBI)$_n$** complexes were further probed by ^{1}H-NMR spectroscopy. Figure-3 illustrates a comparison of the ^{1}H-NMR spectra of **P4VP(PDP-UNBI)$_{1.0}$** with that of neat constituents P4VP and **PDP-UNBI**, all recorded at a concentration of 20 mg/mL in deuterated chloroform ($CDCl_3$) solution at ambient temperature. A broadening of peak was found for all the protons in the 1:1 **P4VP(PDP-UNBI)$_{1.0}$** complex including the aliphatic protons, which is typically found for high molecular weight polymeric materials. The protons that were directly influenced by the hydrogen bonding between phenol group of PDP unit and the ring protons of pyridine unit in P4VP alone are labelled. Of these the pyridine ring protons labelled 'a' and 'b' underwent a deshielded shift from 8.33 to 8.36 ppm and 6.42 to 6.47 ppm respectively which was caused by the involvement of the lone pair of electrons on the nitrogen atom in hydrogen bonding with phenol-OH of **PDP-UNBI**. Another important observation was that the four naphthalene ring protons located around 8.82 ppm moved upfield to 8.76 ppm in 1:1 complex, which gave indirect evidence for the increased extent of association of the naphthalene core, because upfield chemical shift of fused aromatic ring protons occurs as a result of the "ring current" effect generated by neighboring rings in close

proximity as in a self-assembled π-stack.[41-43] The extent of association in **P4VP(PDP-UNBI)$_n$** as a function of 'n' was also studied by proton NMR spectroscopy, where n = 0.25, 0.50, 0.75 and 1.00. Supporting information figure-S.7 shows the expanded aromatic region of the ^{1}H-NMR spectra of **P4VP(PDP-UNBI)$_n$** complexes from 6.00 to 9.00 ppm recorded in $CDCl_3$ at room temperature. The naphthalene core protons in the δ region from 8.78 - 8.87 ppm, were split into multiplets for the complexes **P4VP(PDP-UNBI)$_n$** with imbalanced pyridine to **PDP-UNBI** stoichiometry (n<1), whereas an overall broadened peak was observed for the 1:1 complex pointing towards strong aggregation of the naphthalene cores when each pyridine unit of the polymer chain was associated with one **PDP-UNBI** molecule.

Structural Analysis of the Self-assembled Comb-polymer Complexes

(a) Wide Angle X-ray diffraction studies

Polymeric comb-architectured supramolecules are found to exhibit different self-assembled structures which could be typical lamellar type organization as in the case of homopolymeric comb-complex of P4VP with pentadecylphenol (PDP) or nonadecylphenol (NDP)[33, 44] or ordered hexagonal self-organization obtained as in the case of multi-comb polymer complex of P4VP with $Zn(DBS)_2$ (Zinc-dodecylbenzene sulphonate) and 2,6-bis(octylaminomethyl pyridine) via coordination and electrostatic interactions and so on.[45]

Wide angle X-ray diffraction measurements were conducted to analyze the self-assembled structures formed by the **PDP-UNBI** based supramolecular comb-polymers. Figure-4 shows the XRD trace of the **P4VP(PDP-UNBI)$_{1.0}$** from 2θ = 2-35° and it is compared with that of **P4VP(PDP-UNBI)$_{0.25}$** which had lowest loading of **PDP-UNBI** such that only 25% of the pyridine rings were engaged in hydrogen-bonding at any given instant. The neat constituents P4VP and **PDP-UNBI** are also considered for comparison as a reference. Due to its amorphous nature, neat P4VP exhibited only two broad halos around 2θ values 10° and 20°. The other samples also did not exhibit peaks lower than angle 2θ = 2°.

Generally in the bulk materials the small molecule surfactants undergo ordering at relatively small length scale of approximately 2-5 nm range. The intensity curve of pure **PDP-UNBI** showed a diffraction maximum around 2θ = 4.04° corresponding to the fundamental packing distance of 21.85 Å, calculated using Bragg's equation, nλ = 2dSinθ where λ is the wavelength of X-ray i.e., 1.54 Å, d is the spacing between the reflecting planes and 2θ is the

diffracting angle. For the **P4VP(PDP-UNBI)$_{0.25}$** sample, where only 25 % of the pyridine rings were complexed with **PDP-UNBI**, the packing distance increased slightly to 22.29 Å, whereas the fully complexed **P4VP(PDP-UNBI)$_{1.0}$** sample had a periodicity length around 23.22 Å which was ~1 Å larger than that of the neat **PDP-UNBI**. The layering distance of these supramolecular structures depends upon a delicate balance between the surfactant-polymer interaction and the entropic penalty associated with the polymer chain conformational restrictions imposed upon incorporation of the surfactant molecules to the polymer chains, which otherwise adopt a coiled conformation. Upon attachment of the surfactants by attractive hydrogen-bonding interactions, the polymer chains are proposed to suffer a stiffening of the chains induced by the additional ordering or crystallization of these surfactant molecules which determines the repeat distance of the layers. From the WXRD data it could also be seen that **P4VP(PDP-UNBI)$_{1.0}$** showed almost equally spaced peak patterns typical of microphase separated lamellar phase with Bragg reflections following the ratio 1: 1/2 : 1/3 : 1/4 : 1/5 at 3.80° (23.22Å), 7.76° (11.37Å), 10.25° (8.61Å), 11.89° (7.42Å), 14.42° (6.12Å) respectively. Notably the **PDP-UNBI** small molecule also exhibited similar layered structure; the difference between the two being the different layer spacing values. The detailed calculated and observed interlayer spacing distances (in Å) with the corresponding 2θ values tabulated from the WXRD results are given in table-1. When analyzed carefully it was found that the stoichiometric 1:1 complex **P4VP(PDP-UNBI)$_{1.0}$** had the observed d-spacing values more closer to the perfectly layered structure upto the fifth order diffraction peak confirming lamellar phase with long range orientation and order. Interestingly in the lowest chromophore loaded sample namely **P4VP(PDP-UNBI)$_{0.25}$** the peak corresponding to the second order reflection was found to be completely absent. This provided the hint regarding the existence of some extent of disorder in the system when the un-complexed P4VP domains were more. In particular it proved that in these hydrogen bonded complexes the P4VP and **PDP-UNBI** domains were not macrophase separated. Thus it could be concluded that the **P4VP(PDP-UNBI)$_{1.0}$** complex formed a microphase separated lamellar structure with alternating P4VP and **PDP-UNBI** layers with the overall conformation of each layer being affected by one another in a synergistic manner.

In order to understand further the influence of hydrogen bonding in the overall packing of the complex, a new complex involving P4VP and a non-hydrogen bonded naphthalenebisimide molecule (**EH-SNBI**) – a symmetric NBI derivative having branched ethylhexyl chains

substituted on both imide positions, was prepared. The complex of a 1:1 molar mixture of P4VP and **EH-SNBI,** named **P4VP(EH-SNBI)$_{1.0}$** was prepared under similar experimental conditions as that for **P4VP(PDP-UNBI)** complex. Supporting information figure-S.8 A compares the normalized WXRD patterns for the crystalline **EH-SNBI** (structure given in the figure) with **P4VP(EH-SNBI)$_{1.0}$**. For the sake of comparison a normalized WXRD trace of **PDP-UNBI** and **P4VP(PDP-UNBI)$_{1.0}$** is also given in the figure. When the complex was formed between the symmetric non-hydrogen bondable naphthalenebisimide derivative, no shift was observed in the XRD peak pattern. On the other hand, a clear shift was observed in the WXRD pattern in the case of **P4VP(PDP-UNBI)$_{1.0}$** with the fundamental periodicity length increasing from 21.85 Å in **PDP-UNBI** to 23.22 Å in **P4VP(PDP-UNBI)$_{1.0}$** as discussed earlier. Although similar amounts of P4VP were taken for both experiments, the amorphous signature of P4VP was evident only in the hydrogen bonded complex due to their microphase separation. In the 1:1 **P4VP(PDP-UNBI)$_{1.0}$** complex, the crystallinity of the **PDP-UNBI** molecule was not completely lost as found in the case of conventional covalently connected polymers. The degree of crystallinity calculated for the **P4VP(PDP-UNBI)$_{1.0}$** complex from the XRD data was found to be 64 % and the crystallite size increased from 28.78 nm to 30.90 nm on moving from **PDP-UNBI** to **P4VP(PDP-UNBI)$_{1.0}$** (calculated using Debye-Scherrer formula $t = k\lambda / \beta \cos\theta$).

(b) Single Crystal XRD studies

The molecular conformation of a single surfactant unit is very important, since it determines the overall packing in the bulk structure and the variations thereafter bestowed by hydrogen bonding with P4VP chains. Thus in order to shed more light on the packing motifs in the hydrogen bonded supramolecular polymer complex, single crystals of **PDP-UNBI** small molecule were grown from different solvents like $CHCl_3$, DMF and THF. However irrespective of the solvent used, the crystals formed were extremely thin needle-like and often grew in bunches resulting in poor diffraction data. Optical microscope images of the yellow needle like **PDP-UNBI** crystals grown from saturated DMF solution that were used for single crystal XRD analysis are shown in supporting information figure-S.9. The rigid aromatic cores could easily be solved with good precision, but the long $C_{15}H_{31}$ alkyl chain of the PDP group showed high degrees of flexibility such that it was difficult to fix the electron densities beyond 6th carbon atom of the chain, even when the measurements were conducted at low temperature. The crystallization of **PDP-UNBI** was best indexed on an orthorhombic unit cell with dimensions a = 20.076 Å; b = 49.223 Å; c =

8.695 Å and a molecular length of 14.104 Å along the rigid aromatic cores. The complete crystallographic data for the **PDP-UNBI** molecule is listed in table-S.1 given in supporting information. The crystal structure is shown in figure-5(a) with the hydrogen atoms and the co-crystallized DMF solvent molecules were omitted for clarity. There were eight independent units per cell as visible in figure-5(b). Along the a-axis (i.e., in the c-b plane), the aromatic NBI cores could be found stacked in a typical herringbone like fashion with two nearby independent core planes more or less orthogonal to each other giving rise to a face-to-edge contact pattern (see figure-7(c)). The closest interplanar spacing between neighboring **PDP-UNBI** molecules featured a short vertical distance of 3.369 Å, which correspond to the π-π stacking interactions. Furthermore, in the crystal lattice each **PDP-UNBI** molecule was associated with one DMF (N,N'-dimethylformamide) solvent molecule via hydrogen bonding between the phenolic-OH group of the PDP unit and oxygen atom of carbonyl (CO) group of DMF, as found in the H-bond contacts developed from the crystal packing (Supporting info figure-S.10). In the original crystal lattice of **PDP-UNBI** where no solvent molecules would be present, it could be expected from this packing diagram that the next closest contact for H-bonding would be with the imide carbonyl (CO) group of the neighboring naphthalene ring (indicated in red dotted circles in figure-S.10). Upon complete stoichiometric complexation with P4VP, the fundamental periodicity length increased to 23.22 Å as seen from the XRD data (figure-4). Thus, the main layering distance that got altered by interference by P4VP would be the a-axis along which the **PDP-UNBI** molecules adopted a tilted orientation (figure-6(a)). Therefore the overall packing picture before and after complexation has been envisioned as given in figure-6(b) & (c). The hydrogen bonding of pyridine rings of P4VP chains to the PDP phenol groups of **PDP-UNBI** could be expected to break the previously present phenol-carbonyl (O-H···CO) H-bonding. As a result, the slight increment in layer spacing observed from the XRD data could be rationalized by the change in orientation of the **PDP-UNBI** from tilted to extended rods due to invasion of stretched P4VP chains as illustrated in figure-6(c) with more probability towards a face-to-face packed slipped π-stacking arrangement which is known to exhibit better electronic communication between the active cores compared to typical face-to-edge herringbone packing.[46]

Oriented Lamellar Nanostructures - TEM Imaging

The direct imaging of the microphase separated morphologies formed by the hydrogen bonded supramolecular complexes was investigated by transmission electron microscopic technique (TEM). Very thin films of the bulk samples were first prepared by solution drop casting directly onto copper grids for analysis. The samples were stained with iodine vapors to get images with enhanced contrast.[35, 36] Figure-7 shows the TEM images of the **P4VP(PDP-UNBI)$_{1.0}$** comb-polymer cast from 2mg/mL $CHCl_3$ solution and the corresponding histogram profile is also given. The bright regions are the **PDP-UNBI** and the dark regions corresponded to the P4VP which was preferentially stained by iodine. As anticipated, lamellar nanostructures were observed for the stoichiometrically balanced 1:1 **P4VP(PDP-UNBI)$_{1.0}$** complex. P4VP is a simple homopolymer, which by itself is not known to exhibit any microphase separated lamellar morphology. Therefore the very clear periodic lamellar pattern could be unambiguously originating from the hydrogen bonding induced microphase separation of **P4VP(PDP-UNBI)$_{1.0}$** supramolecular comb polymer architecture. If the self-aggregation of PDP-UNBI was strong enough even in the presence of P4VP, plain macrophase separation of the two domains would occur. This indirectly implies that hydrogen bonding is the decisive criterion leading to the occurrence of such highly ordered lamellar microphase separation. Also the parallel π-π stacking of the perylene chromophore units synergistically assists the hydrogen bonding interactions thus stabilizing the periodic nanostructures. The domain spacing of the **PDP-UNBI** layer obtained from the histogram profile was around 9Å which was close to the molecular length along the rigid part (~ 14 Å). The domain spacings from the TEM images were obtained by averaging over a number of planes and since the TEM pictures are not calibrated the deviation in the periodicities from XRD measurements are always subject to certain error margin.

Charge Transport Properties of the Complexes - SCLC Measurements

The HOMO and LUMO values of **P4VP(PDP-UNBI)$_{1.0}$** was determined as -7.13 eV and -4.05 eV respectively from combined cyclic voltammetry and absorption spectroscopy studies (supporting info S-11). The electron transport characteristics of the hydrogen bonded supramolecular comb polymer was investigated by space-charge-limited current (SCLC) method.[47, 48] The basic device structure consisted of H-bonded supramolecular complex films deposited on ITO coated glass with Aluminium (Al) as the counter electrode. The choice of ITO coated substrates offers a robust surface for deposition. Besides, the ability to inject holes beyond

a threshold voltage, the ITO electrode-substrates have also been used in case of electron-only transport properties, especially for semiconductors where the HOMO level is beyond 5 eV. This presence of barrier for hole injection, when accompanied by LUMO levels which are appropriately located with respect to the cathode (Al in this case), is suitable for measuring SCLC mobility in electron-only device.[49, 50] In the low-voltage regime, electron injection from Al electrode is more effective than hole injection from ITO and the device is largely a unipolar device. The sandwich structure was fabricated by drop casting the 15 mg/ml solution in chloroform on the ITO substrate. Typical thickness, d, of pristine **PDP-UNBI** and **P4VP(PDP-UNBI)$_{1.0}$** complex films were in 3-5 μm range and area of the device defined by the Al electrode was ~ 0.1 cm^2. The top Al electrode was evaporated at the rate of ~ 2 Å/s in a thermal evaporation chamber under 10^{-6} mbar pressure. The electron mobilities were extracted from the J-V curve by fitting to a Mott-Gurney form of behaviour [48]; $J_{sclc} = (9/8)\ \varepsilon\varepsilon_0\mu V^2/d^3$ where J_{SCLC} is the current density in SCLC region, V is the applied voltage, ε and ε_0 are the relative dielectric constant of the organic layer and permittivity of the free space respectively, μ is the charge carrier mobility, and d is the thickness of the organic layer.

Figure-10 (a) & (b) depicts the J(V) responses corresponding to the 1:1 comb-polymer complex **P4VP(PDP-UNBI)$_{1.0}$** and the precursor molecule **PDP-UNBI** respectively. The trend of J with respect to the electric field E (= V/d) are shown in supplementary information (supporting info S-12). For a given system, the J(E) was observed to have similar profile for different thickness. A minimum of three devices were typically measured for each system**;** the statistics for variation of the electron mobility value is given in table 2. The maximum bulk mobility estimate of ~ 9 x 10^{-3} cm^2/Vs of **PDP-UNBI** can be possibly interpreted on the basis of a face-to-edge herringbone type of molecular packing observed from structural studies.[46] This form of packing is not expected to be conducive for long range diffusion of injected charge carriers. On the other hand, the hydrogen bonded polymeric complex **P4VP(PDP-UNBI)$_{1.0}$** exhibits maximum electron mobility of ~ 2 x 10^{-2} cm^2/Vs, which is consistent with the packing model estimation from the structural studies. Upon complexing with P4VP the packing motif of the active **PDP-UNBI** molecules tends towards a face-to-face type stacking arrangement, which facilitates enhanced charge transport. The larger variation in mobility observed in case of **P4VP(PDP-UNBI)$_{1.0}$** as compared to pristine **PDP-UNBI** can then be attributed to the higher sensitivity of the face-on molecular packing to the fabrication-process conditions.

Conclusions

To summarize, the reliable and controllable self-assembly route for preparation of functional n-type semiconducting polymeric materials endowed with highly desirable properties such as crystallinity, processability and high charge transport mobilities for application in optoelectronics like Organic Field Transistors (OFET) was demonstrated in this work. A 3-pentadecylphenol substituted unsymmetric naphthalene bisimide **PDP-UNBI** molecule with phenol head group on one imide position lead to successful complexation with poly(4-vinyl pyridine) P4VP via hydrogen bonding with the nitrogen lone pair of pyridine ring of P4VP. A series of polymer complexes of **P4VP(PDP-UNBI)$_n$** with n = 0.25, 0.50, 0.75 and 1.00 were prepared. Bulk structure analysis using Wide angle X-ray diffraction techniques demonstrated that complexation with P4VP lead to highly ordered layered assembly with improved nanoscale packing of the semiconductor moieties in combination with sufficient solution processability. The packing diagram obtained from the single crystal analysis of the **PDP-UNBI** gave a clear picture of the initial herringbone type arrangement originating from the hydrogen bonding interactions among the self-associated **PDP-UNBI** molecule alone. Correlating this with the X-ray diffraction analyses of the **P4VP(PDP-UNBI)$_{1.0}$** complex provided insight into the probable face-to-face packing of extended crystalline lattice of the **PDP-UNBI** leading to highly ordered lamellar stacks with alternate stretched P4VP layers. The visual evidence for the same was obtained from transmission microscopy (TEM) imaging which confirmed the microphase separated lamellar morphologies. The charge transport properties studied using SCLC technique showed improved electron mobilities of the complex in comparison to the pristine molecule. The present investigation carry forward the message that the concept of supramolecular chemistry applied herewith tunable functionalities and self-organized morphologies leaves open a wide platform for a variety of material applications.

Acknowledgement

This work has been financially supported by the network project NWP0054 and DST Nano Mission project SR/NM/NS-1028/2012. The authors thank Mr. Pankaj from CSIR-NCL, Pune for TEM measurements.

Supporting Information

Synthesis and characterization data for **PDP-UNBI**. Crystallographic data and images.

References

1 H. Minemawari, T. Yamada, H. Matsui, J. Tsutsumi, S. Haas, R. Chiba, R. Kumai, T. Hasegawa, *Nature,* 2011, **475**, 364.

2 K. Takimiya, S. Shinamura, I. Osaka, E. Miyazaki, *Adv. Mater.,* 2011, **23**, 4347.

3 I. Tszydel, M. Kucinska, T. Marszalek, R. Rybakiewicz, A. Nosal, J. Jung, M. Gazicki-Lipman, C. Pitsalidis, C. Gravalidis, S. Logothetidis, M. Zagorska, J. Ulanski, *Adv. Funct. Mater.,* 2012, **22**, 3840.

4 Y. Geng, Shui-Xing. Wu, Hai-Bin. Li, Xiao-Dan. Tang, Y. Wu, Zhong-Min. Su, Y. Liao, *J. Mater. Chem.,* 2011, **21**, 15558.

5 H. Yan, Z. Chen, Y. Zheng, C. Newman, J. R. Quinn, F. Dötz, M. Kastler, A. Facchetti, *Nature* 2009, **457**, 679.

6 F. S. Kim, X. Guo, M. D. Watson, S. A. Jenekhe, *Adv. Mater.*, 2010, **22**, 478.

7 K. Szendrei, D. Jarzab, Z. Chen, A. Facchetti, M. A. Loi, *J. Mater. Chem.,* 2010, **20**, 1317.

8 L. L. Miller, K. R. Man, *Acc. Chem. Res.,* 1996, **29**, 417.

9 H. E. Katz, A. J. Lovinger, J. Johnson, C. Kloc, T. Siegrist, W. Li, Y.-Y. Lin, A. Dodabalapur, *Nature* 2000, **404**, 478.

10 B. A. Jones, A. Facchetti, M. R. Wasielewski, T. J. Marks, *J. Am. Chem. Soc.,* 2007, **129**, 15259.

11 J. H. Oh, Sabin-Lucian. Suraru, Wen-Ya. Lee, M. Könemann, H. W. Höffken, C. Röger, R. Schmidt, Y. Chung, When-Chang. Chen, F. Würthner, Z. Bao, *Adv. Funct. Mater.,* 2010, **20**, 2148.

12 P. Mukhopadhyay, Y. Iwashita, M. Shirakawa, S.-I, Kawano, N. Fujita, S. Shinkai, *Angew. Chem. Int. Ed.,* 2006, **45,** 1592.

13 R. K. Das, S. Banerjee, G. Raffy, A. D. Guerzo, J-P. Desvergne, U. Maitra, *J. Mater. Chem.,* 2010, **20**, 7227.

14 W. Pisula, M. Kastler, D. Wasserfallen, J. W. F. Robertson, F. Nolde, C. Kohl, K. Müllen, *Angew. Chem. Int. Ed.,* 2006, **45**, 819.

15 L. Y. Park, D. G. Hamilton, E. A. McGehee, K. A. McMenimen, *J. Am. Chem. Soc.,* 2003, **125**, 10586.

16 R. S. Lokey, B. L. Iverson, *Nature* 1995, **375**, 303.

17 V. J. Bradford, B. L. Iverson, *J. Am. Chem. Soc.,* 2008, **130**, 1517.

18 H. Y. Au-Yeung, G. D. Pantos, J. K. M. Sanders, *J. Am. Chem. Soc.,* 2009, **131**, 16030.

19 S. A.Vignon, T. Jarrosson, T. Iijima, H. R. Tseng, J. K. M. Sanders, J. F. Stoddart, *J. Am. Chem. Soc.,* 2004, **126**, 9884.

20 G. D. Pantos, P. Pengo, J. K. M. Sanders, *Angew. Chem. Int. Ed.,* 2006, **46**, 194.

21 H. Shao, J. Seifert, N. C. Romano, M. Gao, J. J. Helmus, C. P. Jaroniec, D. A. Modarelli, J. R. Parquette, *Angew. Chem. Int. Ed.,* 2010, **49**, 7688.

22 B. A. Jones, A. Facchetti, T. J. Marks, M. R. Wasielewski, *Chem. Mater.,* 2007, **19**, 2703.

23 D. Shukla, S. F. Nelson, D. C. Freeman, M. Rajeswaran, W. G. Ahearn, D. M. Meyer, J. T. Carey, *Chem. Mater.,* 2008, **20***,* 7486.

24 S.L. Suraru, U. Zschieschang, H. Klauk, F. Würthner, *Chem. Commun.,* 2011, **47**, 11504.

25 Z. Chen, Y. Zheng, H. Yan, A. Facchetti, *J. Am. Chem. Soc.,* 2008, **131**, 8.

26 J. Chen, M.-M. Shi, X.-L. Hu, M. Wang, H.-Z. Chen, *Polymer* 2010, **51**, 2897.

27 C. J. Kudla, D. Dolfen, K. J. Schottler, J.-M. Koenen, D. Breusov, S. Allard, U. Scherf, *Macromolecules* 2010, **43**, 7864.

28 P. Piyakulawat, A. Keawprajak, J. Wlosnewski, M. Forster, U. Asawapirom, *Synth. Met.,* 2011, **161**, 1238.

29 X. Guo, F. S. Kim, M. J. Seger, S. A. Jenekhe, M. D. Watson, *Chem. Mater.,* 2012, **24**, 1434.

30 R. Steyrleuthner, M. Schubert, F. Jaiser, J. C. Blakesley, Z. Chen, A. Facchetti, D. Neher, *Adv. Mater.,* 2010, **22**, 2799.

31 M. Caironi, C. Newman, J. R. Moore, D. Natali, H. Yan, A. Facchetti, H. Sirringhaus, *Appl. Phys. Lett.,* 2010, **96**, 183303.

32 M. Rao, R. P. Ortiz, A. Facchetti, T. J. Marks, K. S. Narayan, *J. Phys. Chem. C* 2010, **114**, 20609.

33 J. Ruokolainen, G. ten Brinke, O. Ikkala, M. Torkkeli, R. Serimaa, *Macromolecules* 1996, **29***,* 3409.

34 B. J. Rancatore, C. E. Mauldin, S.-H. Tung, C. Wang, A. Hexemer, J. Strzalka, J. M. J. Fréchet, T. Xu, *ACS Nano* 2010, **4**, 2721.

35 Cheng-Hao. Yu, Yu-Hao. Chuang, Shih-Huang. Tung, *Polymer* 2011, **52**, 3994.

36 Wei-Han. Huang, Po-Yu. Chen, Shin-Huang. Tung *Macromolecules* 2012, **45**, 1562.

37 R. Narayan, P. Kumar, K. S. Narayan, S. K. Asha, *Adv. Funct. Mater.,* 2013, **23**, 2033.

38 S. W. Kuo, *J. Polym. Res.* 2008, **15**, 459.

39 S. Wu, J. Huang, S. Beckemper, A. Gillner, K. Wang, C. Bubeck *J. Mater. Chem*., 2012, **22**, 4989.

40 K. Kumar, B. Nandan, P. Formanek, M. Stamm. *J. Mater. Chem*., 2011, **21**, 10813.

41 J. Wang, A. Kulago, W, R. Browne, B. L. Feringa, *J. Am. Chem. Soc*., 2010, **132**, 4191.

42 W. Wang, L.-S. Li, G. Helms, H.-H. Zhou, A. D. Q. Li, *J. Am. Chem. Soc.,* 2003, **125**, 1120.

43 J. S. Waugh, R. W. Fessenden, *J. Am. Chem. Soc.,* 1957, **79**, 846.

44 J. Ruokolainen, G. ten Brinke, O. Ikkala, *Adv. Mater.,* 1999, **11**, 777.

45 S. Valkama, O. Lehtonen, K. Lappalainen, H. Kosonen, P. Castro, T. Repo, M. Torkkeli, R. Serimaa, G. ten Brinke, M. Leskelä, O. Ikkala, *Macromol. Rapid Commun.,* 2003, **24**, 556.

46 C. Wang, H. Dong, W. Hu, Y. Liu, D. Zhu, *Chem. Rev.,* 2012, **112**, 2208.

47 M. -A. Muth, M. C. Orozco, M. Thelakkat, *Adv. Funct. Mater.,* 2011, **21**, 4510.

48 A. M. Goodman, A. Rose, *J. Appl. Phys.,* 1971, **42**, 2823.

49 T.-Y. Chu, O. -K. Song, *Appl Phys Lett.*, 2007, **90**, 203512.

50 M.-A. Muth, G. Gupta, A.Wicklein, M. Carrasco-Orozco, T.Thurn-Albrecht, M.Thelakkat, *J Phys. Chem. C* 2013, **118**, 92.

Table-1. Interplanar d-spacing and 2θ values of the layered structures for P4VP(PDP-UNBI)$_n$ (n = 0.25 & 1.00) complexes and PDP-UNBI from the WAXS data recorded at room temperature (25 °C).

Sample	Peak 1		Peak 2		Peak 3		Peak 4		Peak 5	
	2θ (°)	d (Å)	2θ (°)	d (Å)	2θ (°)	d (Å)	2θ (°)	d (Å)	2θ (°)	d (Å)
PDP-UNBI	4.02	21.85	8.01	11.02 (10.93)*	10.04	8.49 (7.28)*	12.08	7.31 (5.46)*	14.60	6.04 (4.37)*
P4VP(PDP-UNBI)$_{0.25}$	3.95	22.29	-	-	11.59	7.60 (7.43)*	14.15	6.24 (5.57)*	17.27	5.11 (4.46)*
P4VP(PDP-UNBI)$_{1.0}$	3.80	23.22	7.76	11.37 (11.61)*	10.25	8.61 (7.74)*	11.89	7.42 (5.81)*	14.42	6.12 (4.65)*

* The values in the bracket correspond to the calculated d-spacing at ratios 1/2, 1/3, 1/4.etc with respect to the fundamental reflection in the case of each sample.

Table 2 Photophysical data of NDI polymers

Sample	Maximum mobility μ_e max (cm^2/Vs)	Average mobility μ_e Avg (cm^2/Vs)	Mean deviation
PDP-UNBI	9.0×10^{-3}	5.6×10^{-3}	$\pm 2.2 \times 10^{-3}$
P4VP(PDP-UNBI)$_{1.0}$	20.0×10^{-3}	9.6×10^{-3}	$\pm 6.6 \times 10^{-3}$

Scheme-1: Chemical structure of **P4VP(PDP-UNBI)$_{1.0}$** supramolecular comb-polymer.

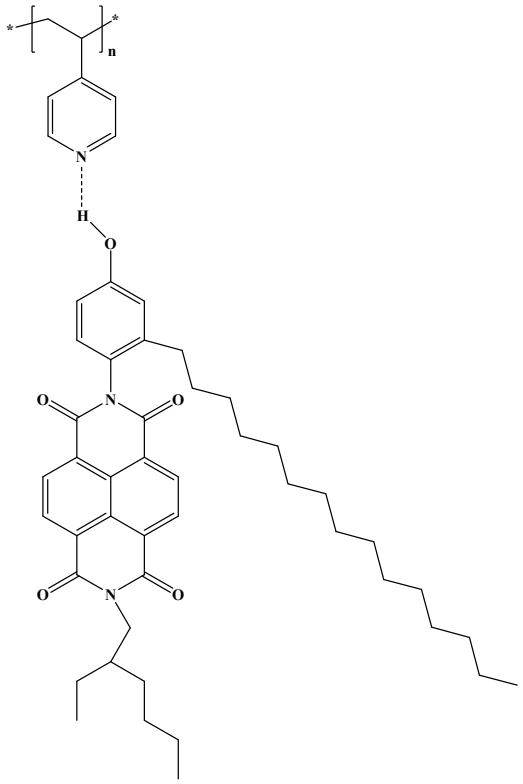

Figure-1. FT-IR spectra of P4VP and **PDP-UNBI** from 4000 to 600 cm^{-1}.

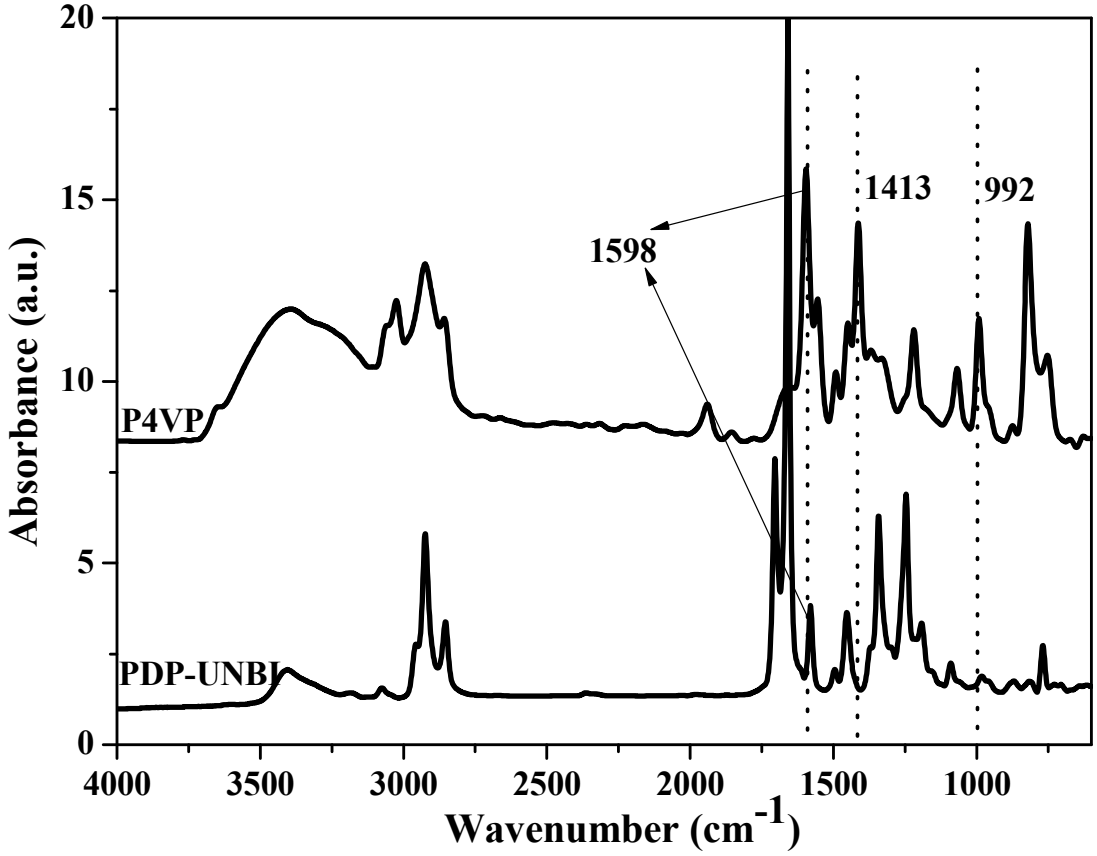

Figure-2. FT-IR spectra of P4VP, **PDP-UNBI** and **P4VP(PDP-UNBI)$_{1.0}$** in the regions (a) 1020 to 990 cm^{-1} and (b) 1430 to 1390 cm^{-1}.

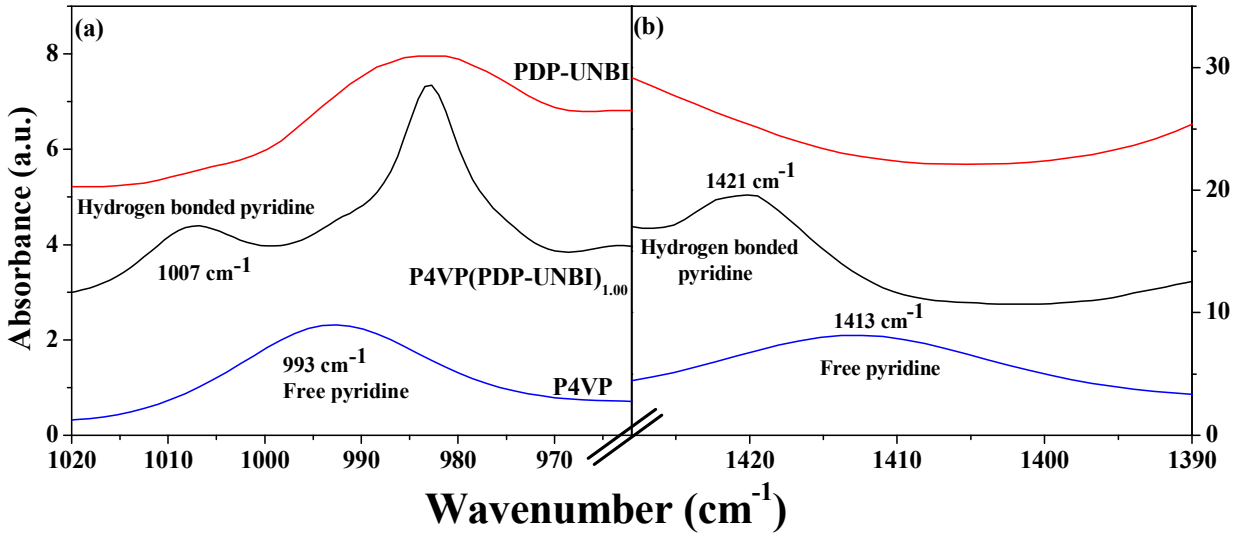

Figure-3. ^{1}H-NMR spectra of (a) P4VP (b) **PDP-UNBI** and (c) **P4VP(PDP-UNBI)$_{1.0}$** recorded in $CDCl_3$ at room temperature.

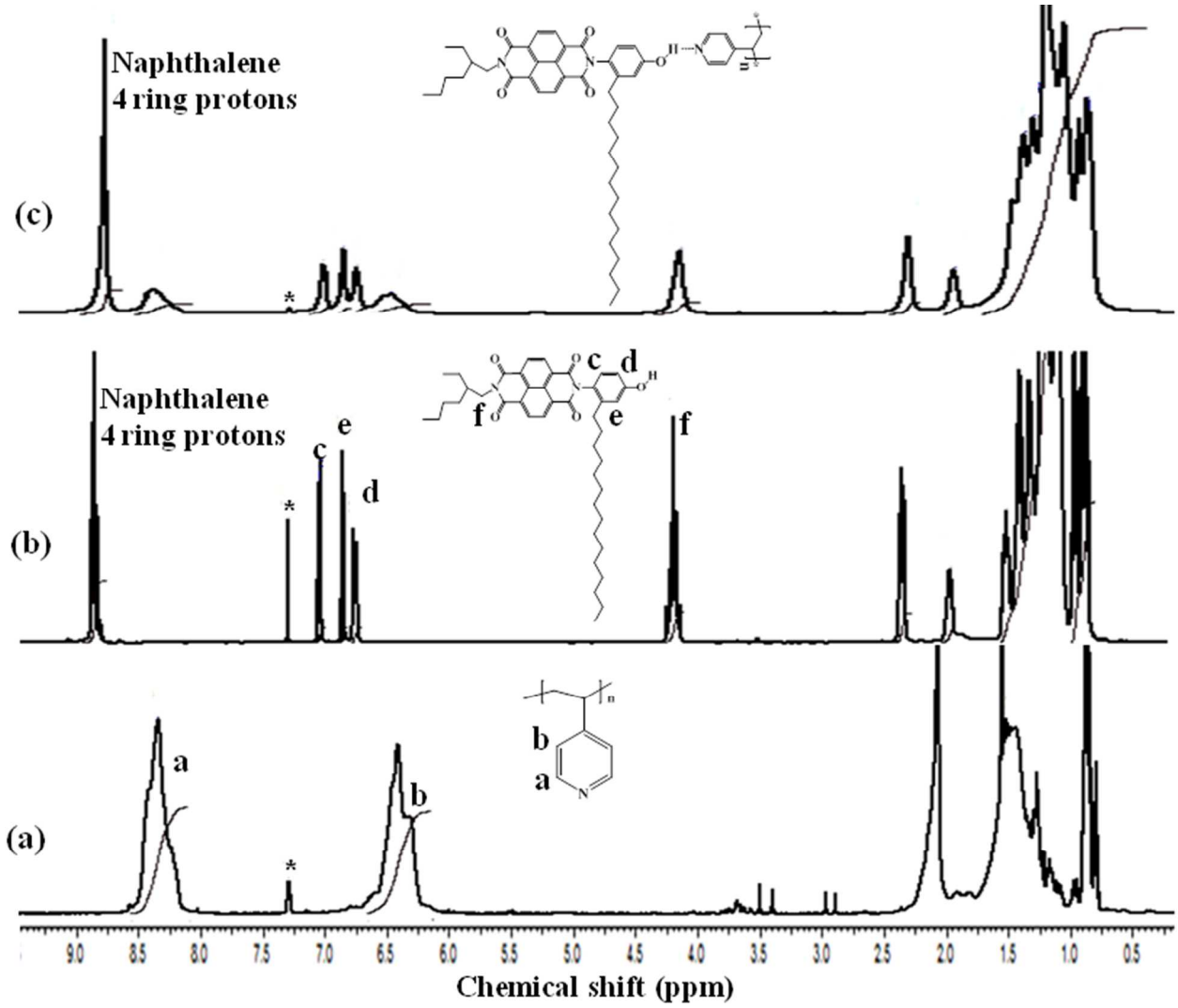

Figure-4. WXRD trace from 2θ = 2 - 35° of **P4VP(PDP-UNBI)$_{1.0}$** compared with that of pure P4VP, **PDP-UNBI** and **P4VP(PDP-UNBI)$_{0.25}$** recorded at room temperature.

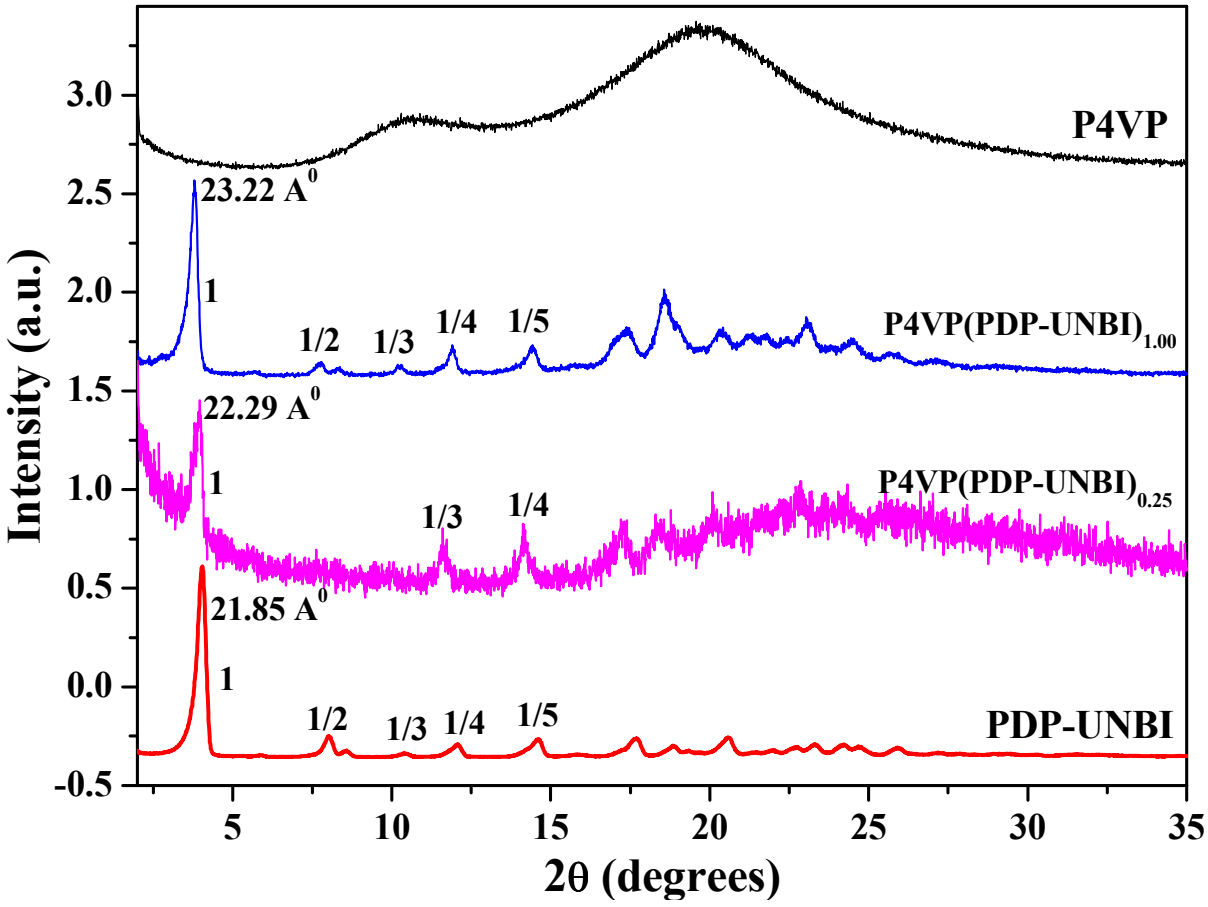

Figure-5. (a) Crystal structure of **PDP-UNBI** (only upto ten carbon atoms of the $C_{15}H_{31}$ chain are shown) with molecular length 14.104 Å along the rigid core. (b) Orthorhombic unit cell structure with 8 molecules per cell. (c) Herringbone stacking of NBI cores with interplanar π-π distance of 3.369 Å viewed along crystallographic a-axis (hydrogen atoms and $C_{15}H_{31}$ alkyl chain omitted for clarity).

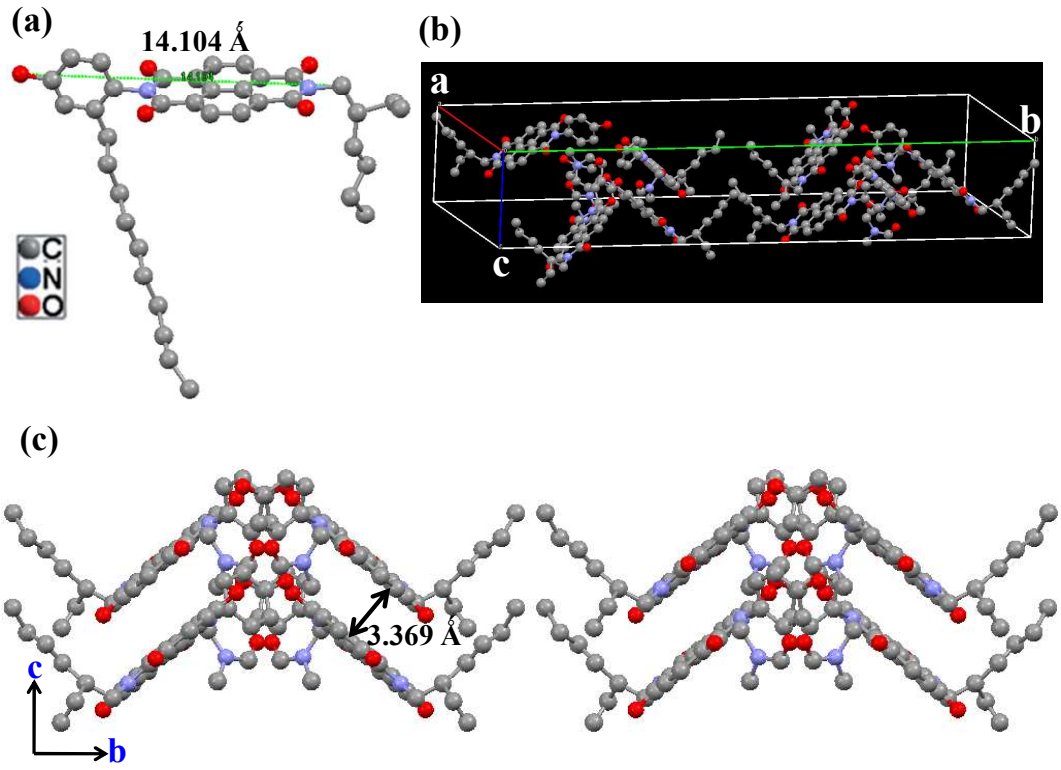

Figure-6. (a) Molecular arrangement of tilted **PDP-UNBI** along a = 20.076 Å. (b) schematic picture showing the P4VP chains attacking the hydrogen bonded sites of **PDP-UNBI** and (c) the resulting change in molecular orientation from tilted to extended rods causing the increase in layer periodicity ($d_2 > d_1$).

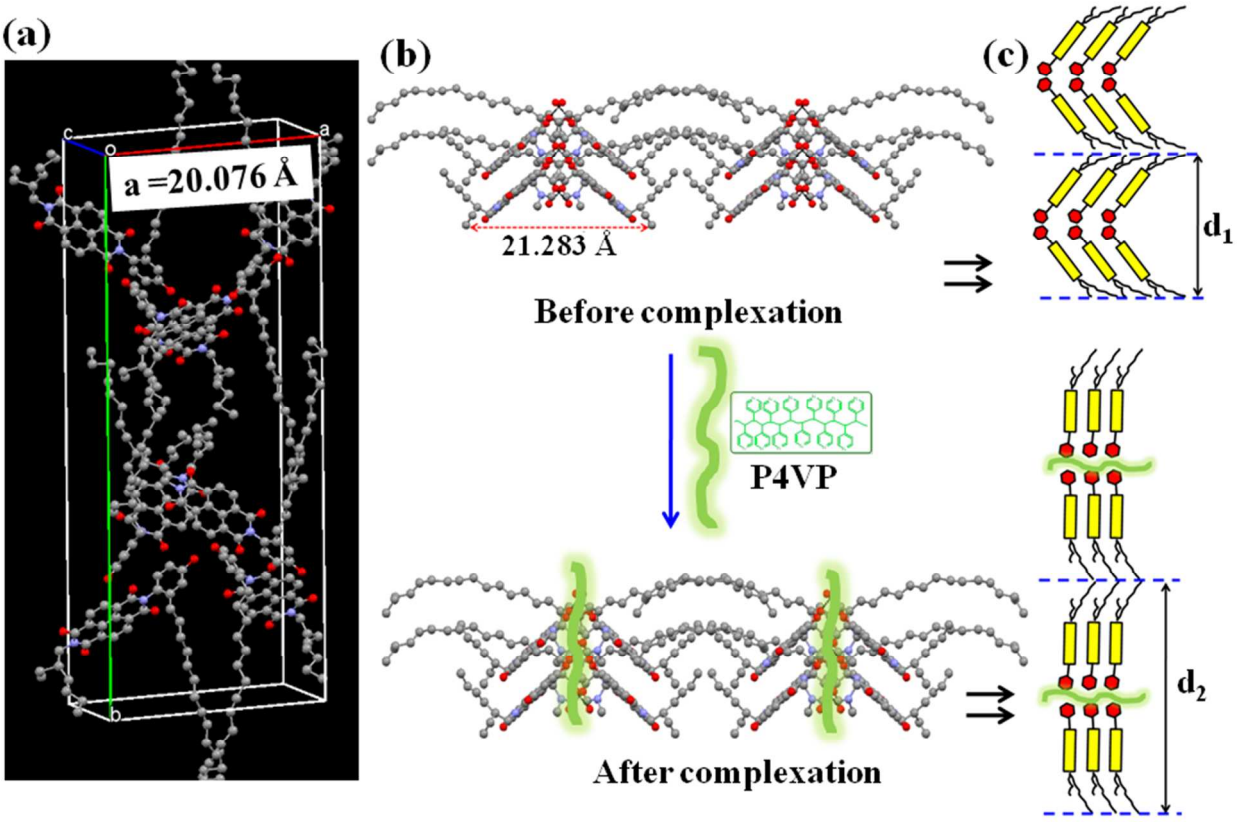

Figure-7. TEM images of **P4VP(PDP-UNBI)$_{1.0}$** homo-comb polymer showing the microphase separated lamellar nanostructures and its histogram .

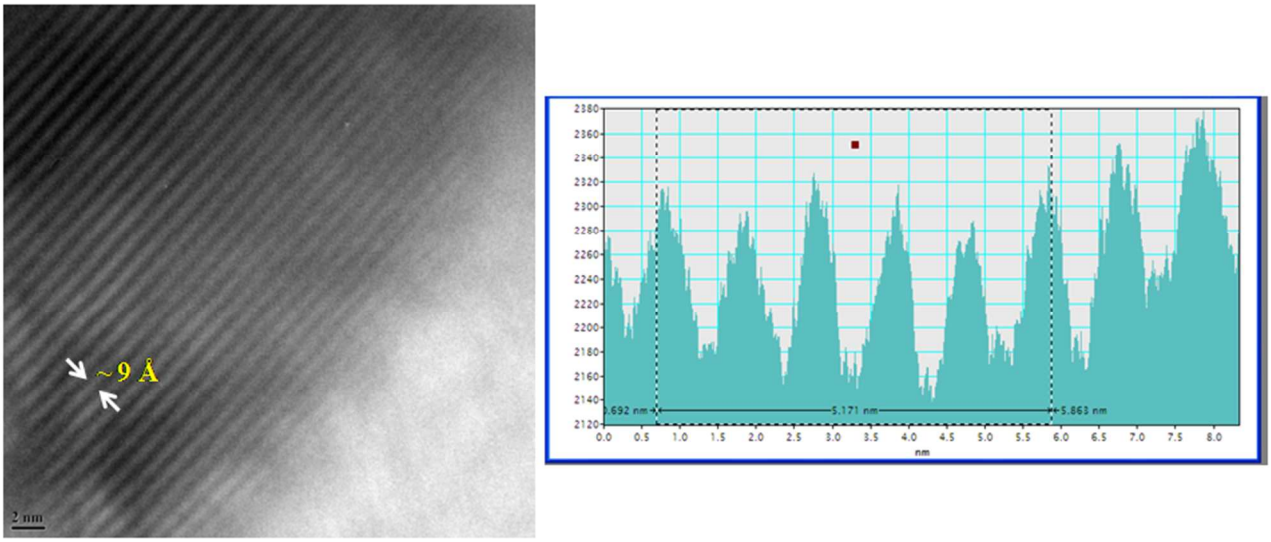

Figure-8. I(V) characteristics of (a) **P4VP(PDP-UNBI)$_{1.0}$** (thickness ~ 5.3 μm, area ~ 0.15 cm^2) and (b) **PDP-UNBI** (thickness ~ 4.4 μm, area ~ 0.094 cm^2) with the solid line indicating the SCLC fit.

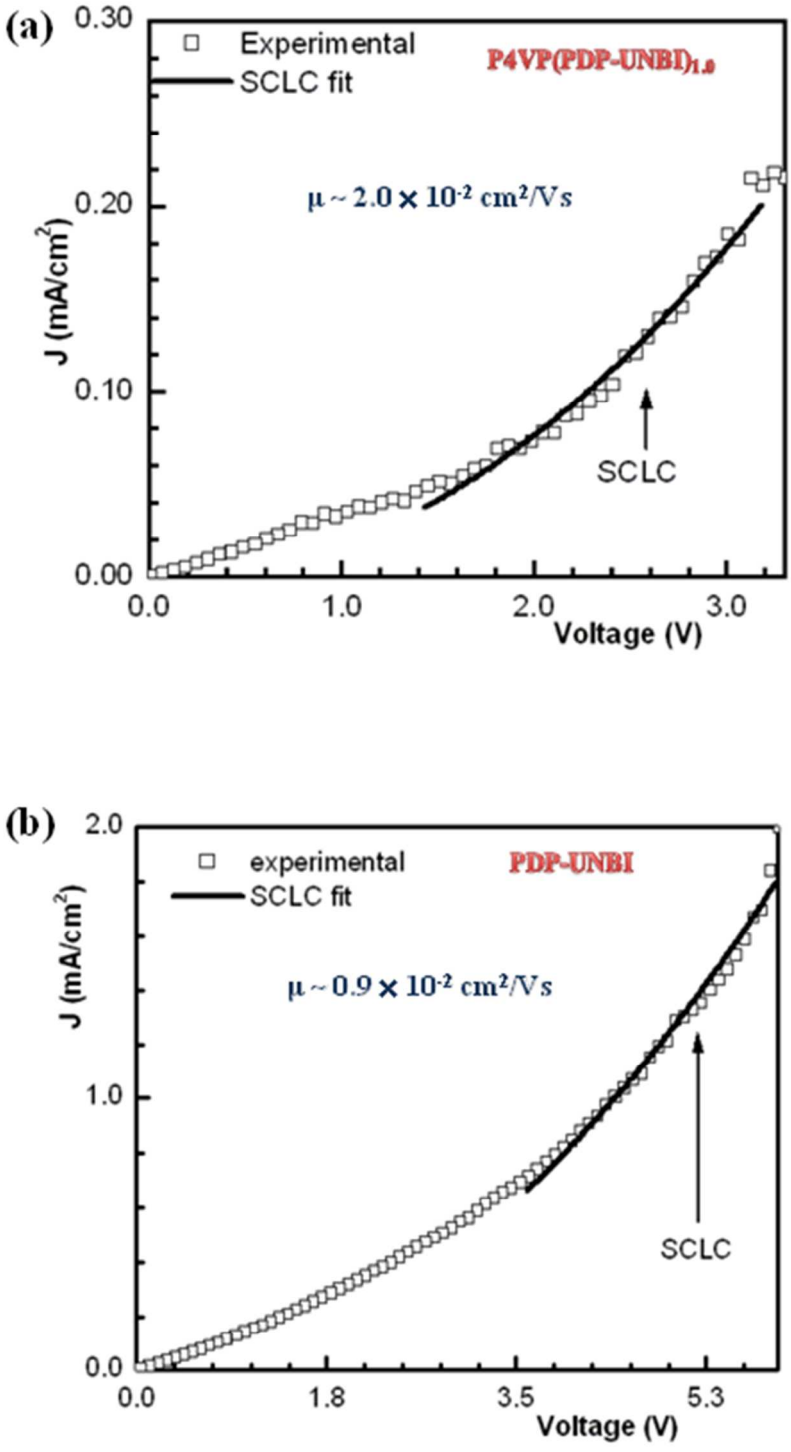

Table of Content

Supramolecular P4VP-Pentadecylphenol Naphthalenebisimide Comb-Polymer: Mesoscopic Organization and Charge transport properties.

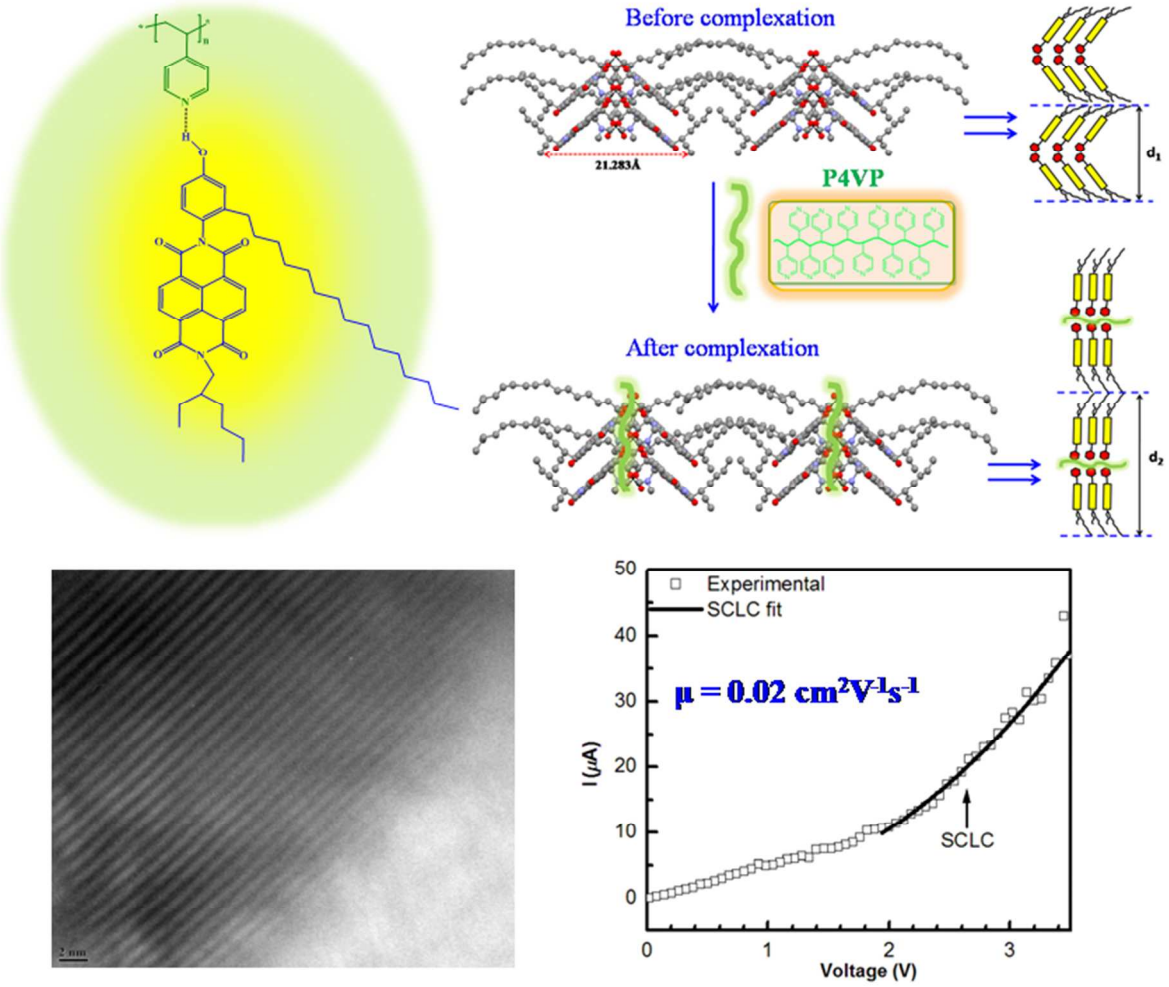

A supramolecular comb polymer complex of unsymmetric naphthalene bisimide **PDP-UNBI** with poly(4-vinyl pyridine) P4VP via hydrogen bonding - **P4VP(PDP-UNBI)$_n$** lead to highly ordered layered assembly with improved nanoscale packing of the semiconductor moieties in combination with sufficient solution processability and improved electron mobilities.